Research on commutation torque ripple suppression strategy of BLDCM based on iterative learning

Jiong Zhang[1]*, Shaofei Chen[2], Lihua Liu[3]

[1]*School of Vocational and Technical Education, Guangxi University of Science and Technology, 268 Dong Huan Road, Liuzhou Guangxi China*

2Engineering Training Center, Guangxi University of Science and Technology, 268 Dong Huan Road, Liuzhou Guangxi China

[3]*College of Science, Guangxi University of Science and Technology, 268 Dong Huan Road, Liuzhou Guangxi China*

Received 4 April 2014, www.tsi.lv

Abstract

Brushless DC motor (BLDCM) is the DC motor which uses electronic commutation instead of mechanical commutation .The torque ripple caused by mechanical structure of the motor is small, while the torque ripple during the commutation is about 50% of the average torque. By analysing the unique features of commutation torque ripple, we can obtain the relationship between the commutation current and torque ripple. The current ripple can be suppressed through adding voltage compensation of the three-phase bridge inverter circuit. Then the commutation torque ripple suppression strategy based on iterative learning was raised in this paper. With the MATLAB Simulink platform, BLDCM simulation models, which based on the iterative learning are established and simulation contrast experiments of open or closed-loop iterative P-type with or without adding the voltage compensation have been designed to test and verify the effectiveness of the suppression strategy.

Keywords: BLDCM, Iterative learning, Torque Ripple, Voltage compensation

1 Introduction

The applied range of brushless DC motor (BLDCM) is becoming wider and wider because of its unique characteristics, such as small size, good performance, simple structure, high reliability, large output torque and so on. However, BLDCM cannot meet a number of occasions with high precision, for it has special problems of commutation torque ripple [1]. Therefore, the suppression of torque ripple is very important to the application of brushless DC motor in high-performance servo system.

Since the torque ripple of BLDCM is affected by electromagnetic factors, motor commutation, cogging effect, armature reaction and mechanical process factors, eliminating the torque ripple needs different methods in accordance with different causes. This paper only focuses on the main factor that causes torque ripple –the commutation. Corresponding voltage compensation is added at the moment of commutation based on characteristics of iterative learning algorithm to weaken the BLDCM commutation torque ripple [2].

2 Mathematical Model of Permanent-Magnet Brushless DC motor (PMBLDCM)

The spatial distribution of magnetic field of BLDCM's rotor is a square wave and the current waveform is also a square wave, while the back-EMF waveform is a 120° trapezoidal wave. In order to simplify the analysis, time-domain equation of state is adopted [3]. And the following assumptions are also made to simplify the analysis:

(1) The stator winding is a 60° full-pitch concentrated winding with star connection.

(2) Eddy current and magnetic hysteresis losses are neglected and magnetic saturation is ignored.

(3) The three-phase windings are completely symmetrical and armature reaction is not considered.

(4) Self-inductance and mutual inductance of the stator winding are constants.

(5) The top width of the air gap magnetic field is 120° electrical angle, the distribution is an approximate rectangular wave and armature reaction is ignored.

(6) The switching characteristics of six power MOSFETS are ideal.

When the three-phase winding with start connection has no neutral line, it does not change with the position change of rotor for the reason of existence of rotor reluctance. Therefore, the coefficients of self-inductance and mutual inductance of stator winding are constants, the voltage balance equation of BLDCM [4-5] is:

$$\begin{bmatrix} u_A \\ u_B \\ u_C \end{bmatrix} = \begin{bmatrix} R_s & 0 & 0 \\ 0 & R_s & 0 \\ 0 & 0 & R_s \end{bmatrix} \begin{bmatrix} i_A \\ i_B \\ i_C \end{bmatrix} + \begin{bmatrix} L_s - L_m & 0 & 0 \\ 0 & L_s - L_m & 0 \\ 0 & 0 & L_s - L_m \end{bmatrix} p \begin{bmatrix} i_A \\ i_B \\ i_C \end{bmatrix} + \begin{bmatrix} e_A \\ e_B \\ e_C \end{bmatrix}, \quad (1)$$

* ***Corresponding author*** e-mail:860454913@qq.com

where: u_a, u_b, u_c - winding voltage of each stator phase (V), i_a, i_b, i_a - winding current of each stator phase (A), e_a, e_b, e_c - winding EMF of each stator phase (V), *R* - resistance of each stator phase (Ω), *L*- self-inductance of each phase winding of the stator (H), *M* - mutual inductance between any two phase windings of the stator (H), *P* - differential operator. The electromagnetic torque equation is as below:

$$T_e = \frac{e_A i_A + e_B i_B + e_C i_C}{\omega / n_p}, \qquad (2)$$

where ω is the mechanical angular velocity of the rotor, T_e is the electromagnetic torque, n_p is the number of motor pole pairs.

3 Analysis of Ripple Torque

3.1 ANALYSIS OF THE COMMUTATION PROCESS

This paper only analyses non-overloaded commutation torque ripple problem [7-8], which meets the condition that $E > 0.25\alpha V$. Where E the back-EMF of the motor is, αV is the actual line voltage of the motor. It is assumed that the power supply voltage of the motor is constant during the entire running process. The equivalent circuit and bridge inverter circuit diagrams of BLDCM can be obtained by the formula (1) and they are shown in Figure 1-5.

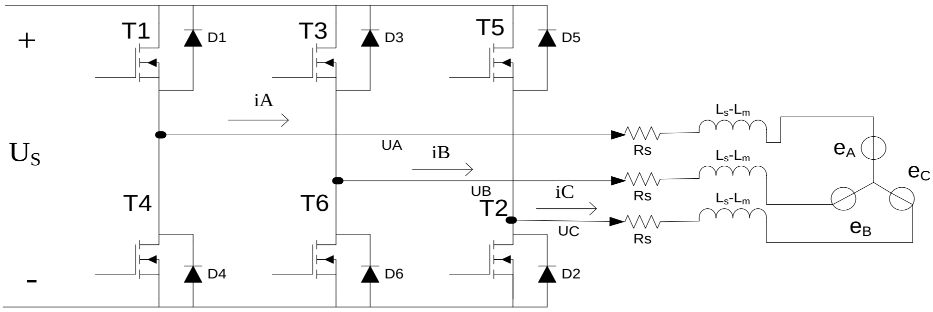

FIGURE 1 The equivalent circuit and bridge inverter circuit diagrams of BLDCM

where Us is the supply voltage at DC side. T1-T6 are switching power Mosfets, D1-D6 are freewheeling diodes. UA, UB and UC are phase voltages of phase A, B and C respectively. iA, iB and iC phase currents of phase A, B and C respectively. Rs is interphase resistance. Ls-Lm is interphase inductance. eA, eB and eC are electromotive forces of phase A, B and C. In this paper, we take the following case for example: the power supply of the motor changes from A-C phases to B-C phases.

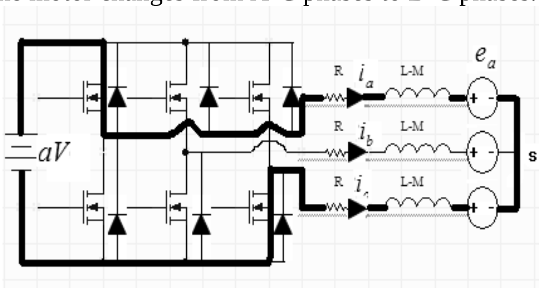

FIGURE 2 Single-current mode before commutation

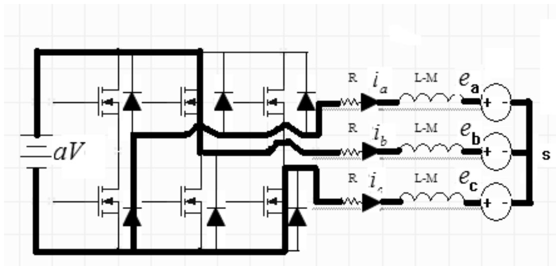

FIGURE 3 Current change mode during phase commutation

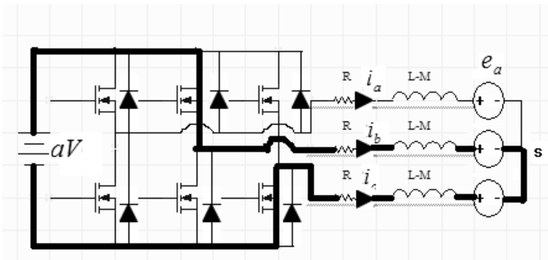

FIGURE 4 Mode after commutation

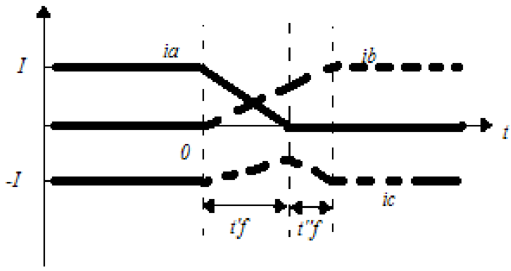

FIGURE 5 Current changes during the commutation process

3.2 CALCULATION OF COMMUTATION CURRENT

It can be found through the above analysis that the current commutation cannot be completed instantaneously in the commutation process due to the presence of inductance in armature winding. The current shutdown is delayed and needs the help of freewheeling diodes [9].

According to the Kirchhoff's law, the influence of motor winding resistance on the commutation project is neglected because it is very small, and the circuit equation is:

$$\begin{cases}(L_s - L_m)pi_A + e_A - ((L_s - L_m)pi_C + e_C) = 0 \\ (L_s - L_m)pi_B + e_B - ((L_s - L_m)pi_C + e_C) = U_s \\ i_A + i_B + i_C = 0\end{cases} \cdot \quad (3)$$

The waveform of back-EMF (back electromotive force) of each phase is a trapezoidal wave with top width of 120° electrical angle, i.e. $e_A = e_B = -e_C = E$. Considering that the initial and final values of each phase current are steady-state values before and after the commutation, the solution of Equation 3 is:

$$\begin{cases} i_A = I_P - \dfrac{Us + 2Ep}{3(Ls - Lm)} t \\ i_B = \dfrac{2(Us - Ep)}{3(Ls - Lm)} t \\ i_C = -I_p - \dfrac{Us - 4Ep}{3(Ls - Lm)} \end{cases}, \quad (4)$$

where I_P represents the steady-state value of the phase current.

3.3 RELATIONSHIP BETWEEN COMMUTATION CURRENT AND TORQUE

The three different situations in Figure 6 can be obtained based on the relations of the amplitude of i_A, i_B and i_C in formula (4).

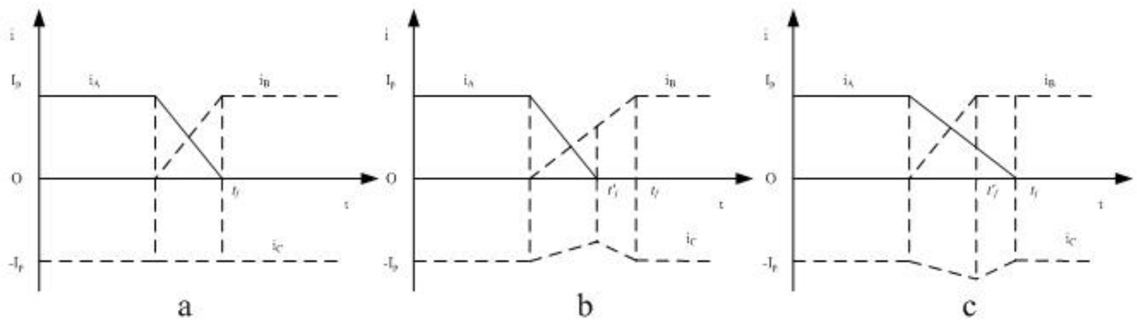

FIGURE 6 Relationship of the Commutation Current of BLDCM

(1) As shown in Figure 6 (a), i_B reaches steady state value, while i_A reduces to 0. Commutation time of A phase winding and B phase winding can be obtained by the formula (4), and they are equal. That is, the two phases will complete the commutation simultaneously, if they meet the following conditions:

$$U_s = 4E_p . \quad (5)$$

Since $i_A + i_B + i_C = 0$, the electromagnetic torque equation of commutation in process can be derived from formula (2) as below:

$$T_e = -\frac{2E_p}{\omega / n_p} i_c = \frac{2E_p}{\omega / n_p}(I_p + \frac{U_s - 4E_p}{3(L_s - L_m)} t) \quad (6)$$

Thus, the electromagnetic torque during commutation is proportional to the current of non-commutation phase winding. The electromagnetic torque during non-commutation period is generated by the interaction effect of synthetic MMFs of two phases and rotor permanent MMFs. It is shown as follows:

$$T_e = -\frac{2E_p}{\omega / n_p} I_p \quad (7)$$

By Equation (5), $U_s = 4E_p$, then:

$$T_e = T_e^{'} - \frac{2E_p}{\omega / n_p} I_p . \quad (8)$$

So there is no torque ripple during the commutation process of BLDCM and this is an ideal work situation. The mechanical characteristic equation of BLDCM is:

$$n = \frac{U_s - 2\Delta U}{C_e \Phi_\delta} - \frac{2R_s}{C_e \Phi_\delta} I_i = \frac{U_s - 2\Delta U}{C_e \Phi_\delta} - \frac{2R_s}{C_T C_e \Phi_\delta^2} T_e , \quad (9)$$

where ΔU - Saturation voltage of power Mosfet, I_i - current of each phase winding, Φ_δ — magnetic flux per pole of corresponding square-wave air gap magnetic induction intensity, C_e - Electrical potential constant, C_T - Torque constant.

(2) As shown in Figure 6 (b), i_B has not reached its steady state value when i_A reduces to 0.

Similarly, it can be seen that the commutation of Figure 6(b) meets the following conditions:

$$U_s < 4E_p . \quad (10)$$

Formulas (6) and (7) show that at this moment. The electromagnetic torque in commutation process is lower than the electromagnetic torque in non-commutation period. That is, commutation causes torque to decrease.

(3) As shown in Figure 6 (c), i_A has not reduced to 0 when i_B reaches its steady state value.

Similarly, it can be obtained that the commutation situation in Figure 6 (c) is opposite to that in Figure 6 (b). The electromagnetic torque in commutation process is bigger than the electromagnetic torque in non-commutation period. That is, commutation causes torque to increase.

4 Control Theory of Iterative Learning

4.1 MATHEMATICAL DESCRIPTION OF ITERATIVE LEARNING

Iterative learning control [10-11] (referred to as IILC) is a branch with strict mathematical description of intelligent control systems. It allows objects to track a desired trajectory with given accuracy within a given time zone, and it does not need identification of system parameters in the running process of the controller. Its mathematical description is as follows:

$$\left.\begin{aligned} \dot{x}(t) &= f(t, x(t), u(t)) \\ y(t) &= g(t, x(t), u(t)) \end{aligned}\right\}, \tag{11}$$

where $x(t) \in \mathrm{R}^{m\times l}$ represent system state vectors, $y(t) \in \mathrm{R}^{m\times l}$ represent the output vectors of the system, $u(t) \in \mathrm{R}^{m\times l}$ are the control vectors, f and g are vector functions of corresponding dimensions.

4.2 COMMUTATION TORQUE RIPPLE SUPPRESSION STRATEGY BASED ON ITERATIVE LEARNING

It can be obtained from section 2.3 that Us=4E must hold if no ripple is allowed during commutation. Positive voltage compensation is carried out when Us <4E and negative voltage compensation is carried out when Us>4E. Torque ripple is actually current ripple. That is, during commutation, negative voltage compensation shall be employed when the detected current exceeds a certain value and positive voltage compensation shall be employed when the detected current is lower than a certain value so as to achieve the purpose of suppressing the torque ripple [12].

Iterative learning control algorithm is used as the speed controller. In addition, open and closed loop P-type iterative torque ripple suppression with voltage compensation and open and closed loop P-type control without voltage compensation are compared with each other to verify the effectiveness of this strategy. The diagram of open-loop P-type iterative torque ripple suppression with voltage compensation is shown in Figure 7. The diagram of closed-loop P-type iterative torque ripple suppression with voltage compensation is shown in Figure 8.

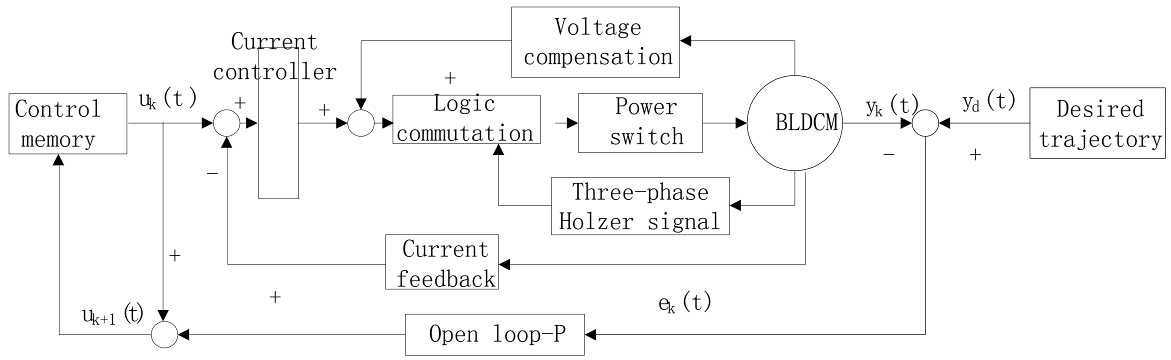

FIGURE 7 torque ripple suppression diagram of open-loop iterative P-type with voltage compensation

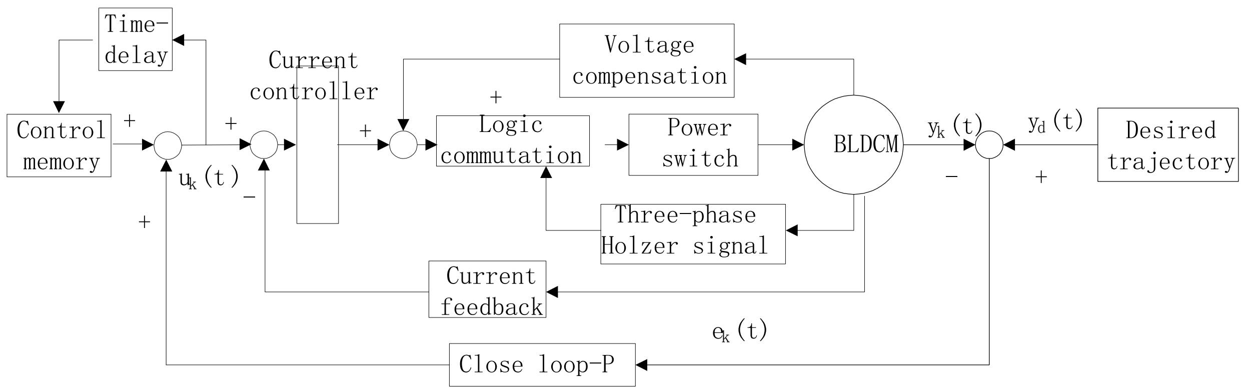

FIGURE 8 torque ripple suppression diagram of closed-loop iterative P-type with adding voltage compensation

5 Simulation of BLDCM Commutation Torque Ripple Suppression

5.1 SIMULATION MODEL OF DOUBLE CLOSED-LOOP CONTROL OF BLDCM

The simulation platform in this paper is MATLAB. Typical dual closed-loop control system of BLDCM is used and simulation parameters are set according to the data book of disc BLDCM provided by Maxon. Every independent sub-module is modelled separately according to the idea of modular modelling [13]. Four simulation models open and closed-loop P-type iteration without adding voltage compensation and open and closed-loop P-type iteration with adding voltage compensation are designed according to the commutation torque ripple suppression strategy based on iterative learning in section 3.

When the given velocity is 1000n/min, the given load is 0.03mNm and t ϵ [0, 0.2], the initial conditions of the system are $u_0(t)=$ y_d (t) and $u_0(t)=y_d(t)$, $y_d(t)=\begin{cases}0 & t<0.1\\ 1000 & t>=0.1\end{cases}$.

(1) Open-loop iterative P-type control without adding voltage compensation

(2) Closed-loop iterative P-type control without adding voltage compensation

(3) Open-loop iterative P-type control with adding voltage compensation

(4) Closed-loop iterative P-type control with adding voltage compensation

Open-loop P-type iterative simulation model without adding voltage compensation is shown in Figure 9, Close-loop P-type iterative simulation model without adding voltage compensation is shown in Figure 10, Open-loop P-type iterative simulation model with adding voltage compensation is shown in Figure 11,Close-loop P-type iterative simulation model with adding voltage compensation is shown in Figure 12.

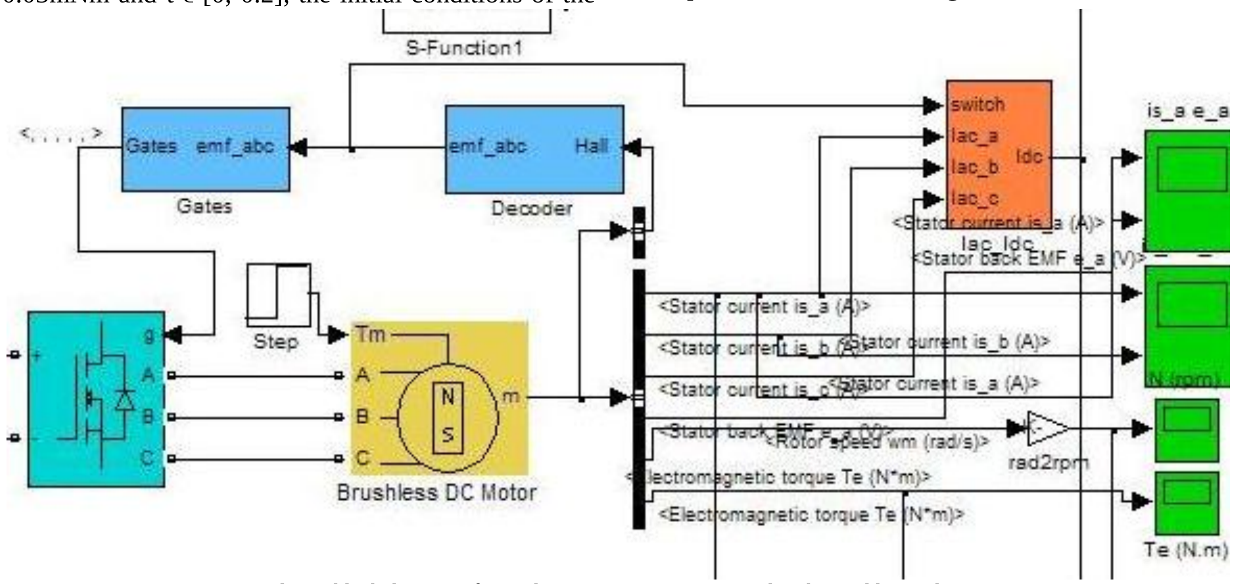

FIGURE 9 Simulation block diagram of open-loop iterative P-type control without adding voltage compensation

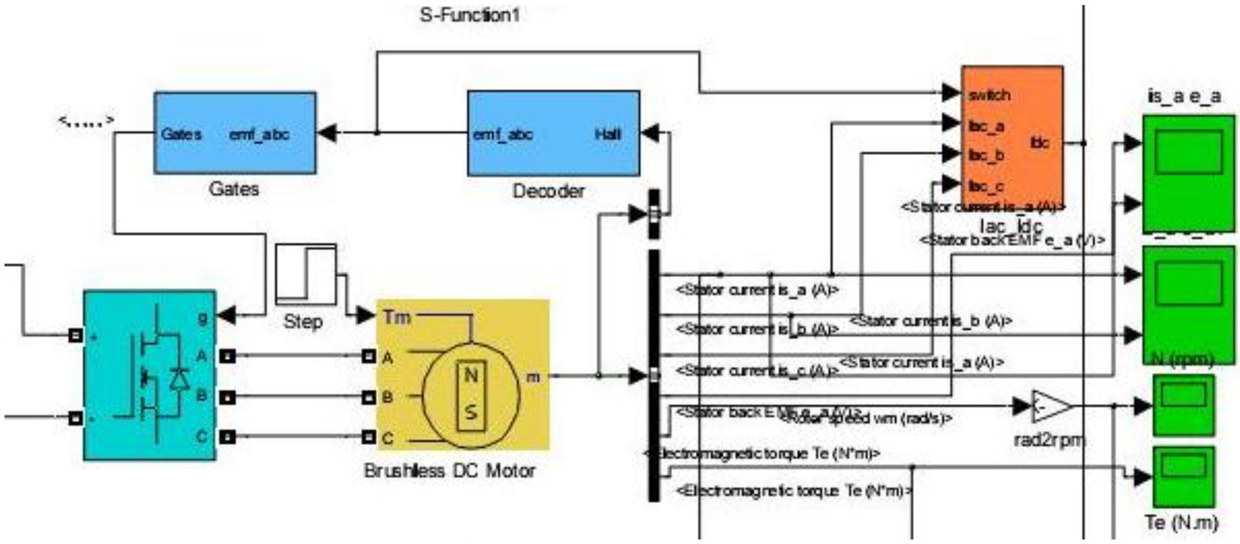

FIGURE 10 Simulation block diagram of the closed-loop iterative P-type control without adding voltage compensation

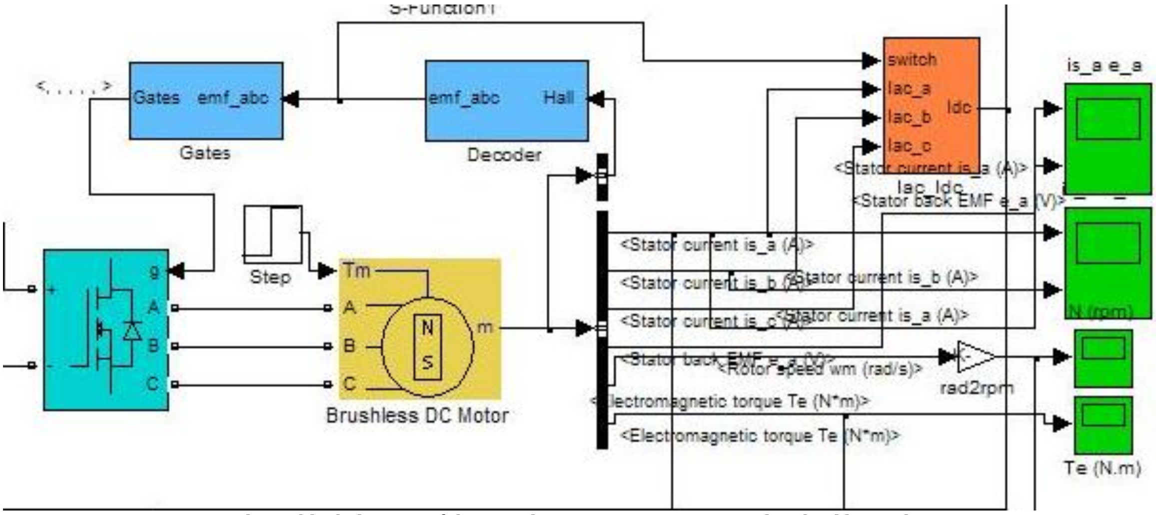

FIGURE 11 Simulation block diagram of the open-loop iterative P-type control with adding voltage compensation

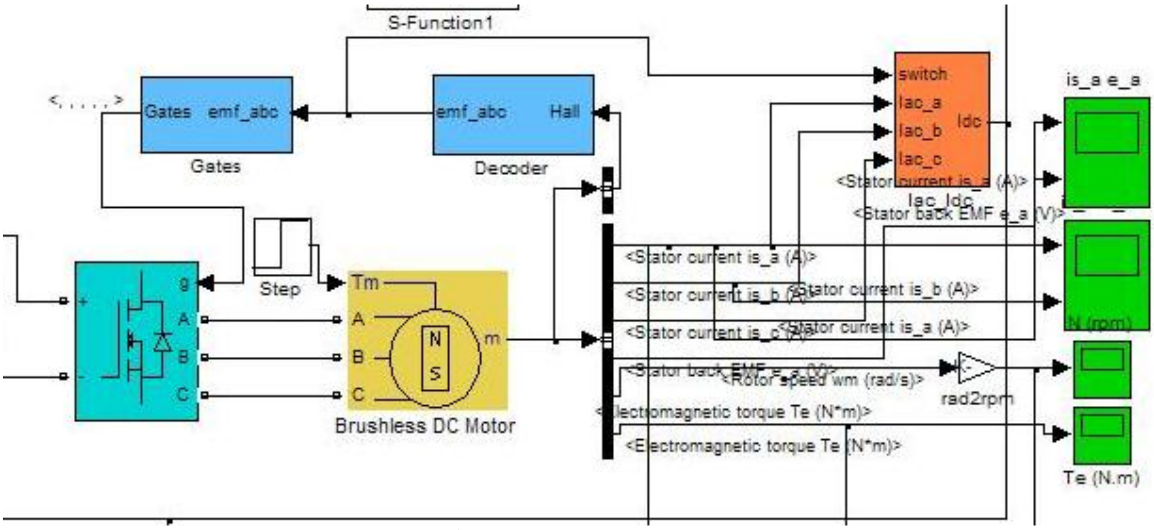

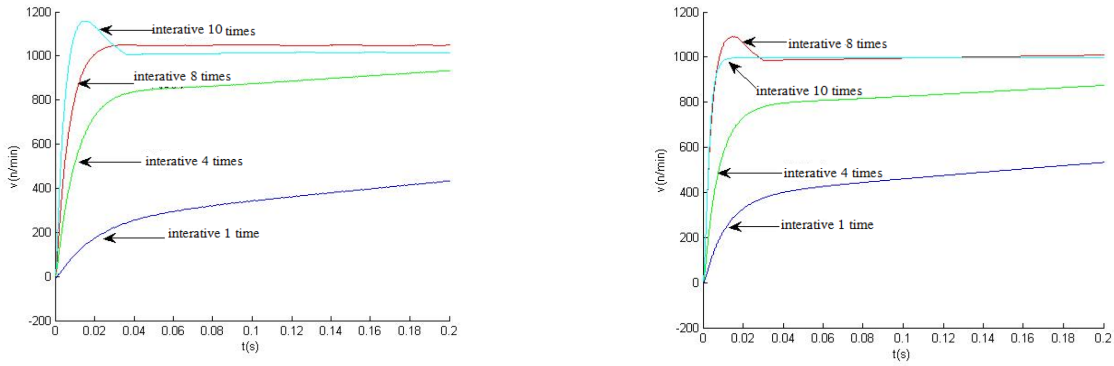

FIGURE 12 Simulation block diagram of the closed-loop iterative P-type control with adding voltage compensation

(a) Open loop (b) Closed loop

FIGURE 13 Speed waveform of open-loop iteration P-type control without adding voltage compensation

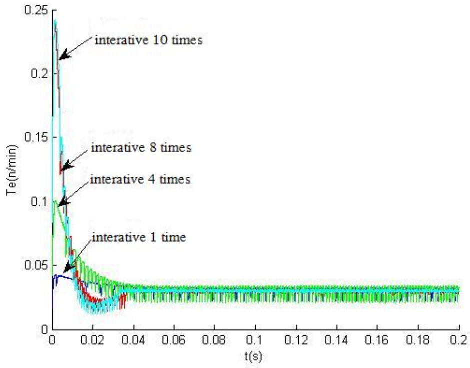

(a) Open loop control without adding voltage compensation

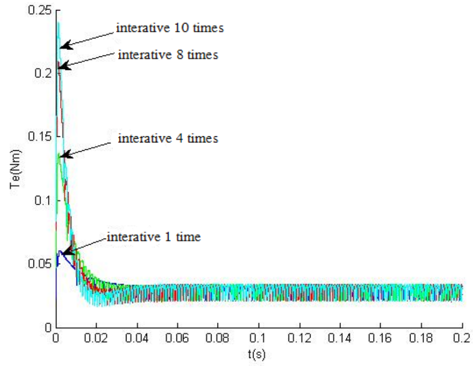

(b) Closed loop control without adding voltage compensation

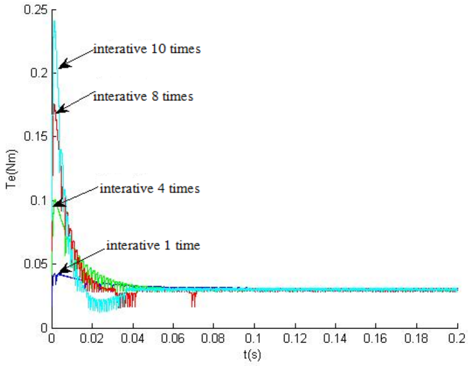

(c) Open loop control with adding voltage compensation

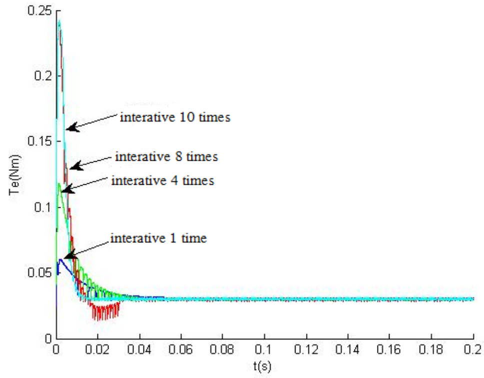

(d) Closed loop control with adding voltage compensation

FIGURE 14 Torque ripple diagram of iterative P-type control

5.2 SIMULATION ANALYSIS

(1) Comparison between open- loop and closed-loop P-type iterative control method

From the comparison between (a) and (b) in the Figure 13, it can be seen that the step response of the control system under closed loop at 10th iterative learning step almost has no overshoot and is much faster than that of control system under open loop control.

By the comparison of Figure 4.13 and Figure 4.16, it can be seen that the step response of the control system under closed loop iterative learning at 10th iterative learning step almost has no overshoot and is much faster. The related parameters comparison is shown in Table 1, open loop P-type iterative control: overshoot σ%=18%, rise time t_r=0.018s，Setting time t_s=0.024s. closed-loop P-type iterative control: overshoot σ%=0%, rise time t_r=0.011s, setting time t_s=0.011s

TABLE 1 Parameters compare of two control methods

Dynamic Performance / Control Method	σ%	t_r	t_s
open- loop P-type	18%	0.018	0.024
closed-loop P-type	0%	0.011	0.011

(2) In closed-loop P-type iterative control, comparison between torque ripple with adding voltage compensation control and torque ripple without adding voltage compensation control is shown in Table 2. By the comparison of four pictures in Figure 14, it can be seen that the torque fluctuation range without adding voltage compensation is [0.02, 0.033] and the torque fluctuation range with adding voltage compensation is [0.029, 0.0312]. The torque ripple drops to 4% from 33.3 %.

The torque ripple partial enlarged drawing of closed loop iteration P-typed control without adding voltage compensation is shown in Figure 15. The torque ripple partial enlarged drawing of closed loop iteration P-typed control with adding voltage compensation is shown in Figure 16.

TABLE 2 Comparison of with and without adding voltage compensation

Dynamic Performance / Control Method	torque fluctuation range	torque fluctuation percentage
With voltage compensation	[0.02, 0.033]	33.3%
with voltage compensation	[0.029, 0.0312]	4%

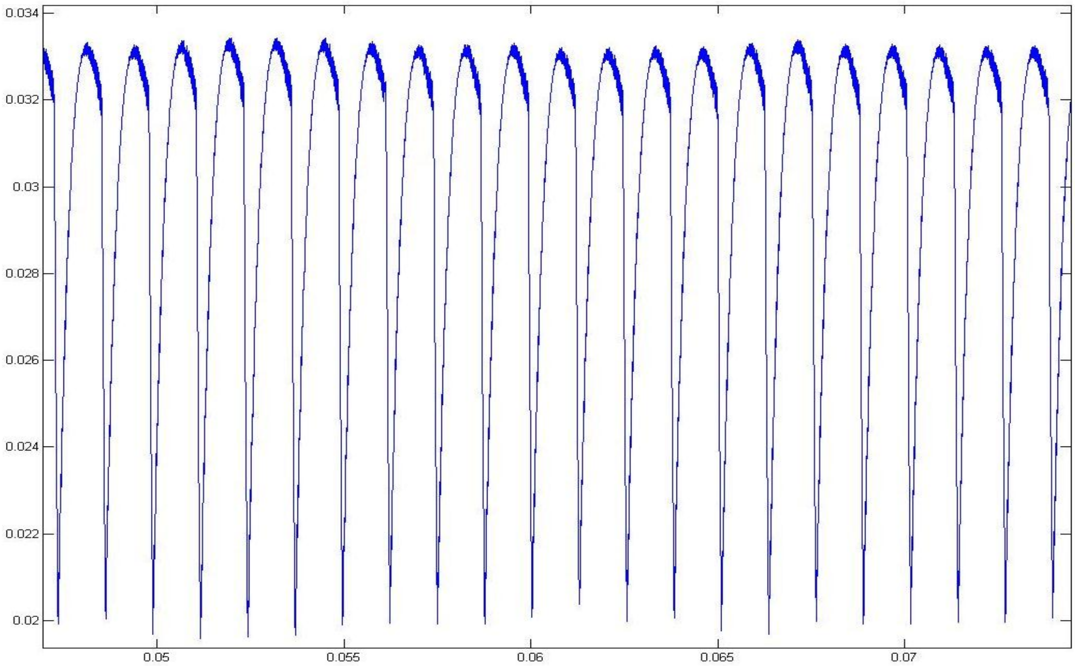

FIGURE 15 Torque ripple partial enlarged diagram of closed-loop iterative P-type control without adding voltage compensation

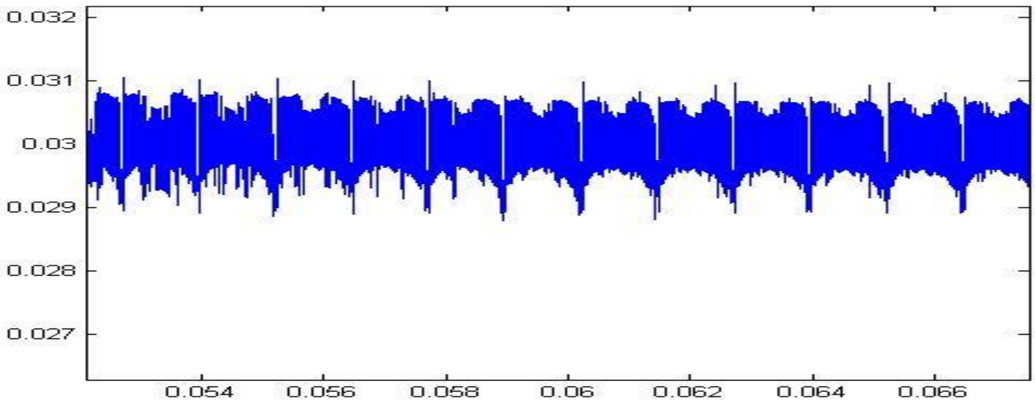

FIGURE 16 Torque ripple partial enlarged diagram of closed-loop iterative P-type control with adding voltage compensation

By analysing the above simulation experiments, it is obtained that the speed control performance of BLDCM under closed-loop iterative P-type control is better than that under open-loop P-type iterative control. With adding voltage compensation to the commutation torque ripple, the torque ripple drops to 4% from the original 33.3%. It means that the torque ripple with adding voltage compensation is greatly restrained. It verifies the effectiveness of commutation torque ripple suppression strategy of BLDCM based on iterative learning control [14-15].

6 Conclusions

Commutation torque ripple is the main factor that restricts the applications of permanent magnet brushless DC motor in high performance alternating current governor systems. Therefore, this paper takes commutation torque ripple of BLDCM as the research object, obtains the relationship between the commutation current and the torque ripple through the analysis of the commutation process and the calculation of commutation current and raises the commutation torque ripple suppression strategy based on the iterative learning. This strategy is realized by adding voltage compensation during commutation of BLDCM based on the detected conditions of current ripple. Through the design of four simulation models and analysis of simulation experimental data, it is obtained that the torque ripple reduces to 1/8 of its previous level by adding voltage compensation during commutation and the effectiveness of commutation torque ripple suppression strategy of BLDCM based on iterative learning is therefore verified.

References

[1] Zwahlen R, Chang T 2007 Feed forward Speed Control of Brushless DC Motors with Input Shaping The 33rd Annual Conference of the *IEEE Industrial Electronics Society(IECON)* 1169-74
[2] Zhao Yao, Wang Huizhen, Chen Kang 2013 A Study About the Control System of BLDCM *Transactions of China Electrotechnical Society* **28**(1) 321-5
[3] Liu Dongliang, Cui Yanfei,Chen Meibin 2013 Research of Back-EMF Estimation for Brushless DC Motor Transactions of *China Electrotechnical Society* **28**(6) 52-8
[4] Peng Bing, Xia Jiakuan,Wang Chengyuan, Jing Rubao 2012 Analysis and Calculation of Zigzag Leakage Flux in Surface-Mounted PM Synchronous Machines with Similar Number of Poles and Slots *Transactions of China Electrotechnical Society* **27**(1) 114-8
[5] He Hucheng, Liu Weiguo, Lang Baohua 2007 Research on Torque Characteristic of Non-commutation in PM Brushless DC Motor. *Electric Drive* **37**(10) 114-8
[6] Pandit M, Buchheit K H 1999 Optimizing Iterative Learning Control of Cyclic Production Process with Application to Extrucers *IEEE Trans* **7**(3) 382-90
[7] Zhu Chi, Aiyama Yasumichi, Arai Tamio, Kawamura Atsuo 2006 Positioning in Releasing Manipulation by Iterative learning Control *Journal of Intelligent and Robotic Systems* **46**(4) 383-404
[8] Sun Mingxuan, Wang Danwei 2000 Iterative learning Control Design for Uncertain Dynamic Systems with Delayed States *Dynamics and Control* **10**(4) 341-57
[9] Ionel D M, Eastham J F, Betaer T 1995 Finite element analysis of a novel brushless DC motor with flux barriers, Magnetics *IEEE Transactions on* **31**(6) 3749-51
[10] Jeon Y S, Mok H S, Choe G H, Kim D K, Ryu J S 2000 A new simulation model of BLDC motor with real back EMF waveform, *Computers in Power Electionics* the 7th Workshop on 16-18 July 2000 217-20
[11] Zhu Z Q, Howe D 2000 Influence of design Parameters on togging torque in permanent magnet machines *IEEE Trans on Energy Conversion* **43**(5) 407-11
[12] Dai Min, Keyhani Ali, Sebastian Tomy 2001 Torque ripple analysis of a permanent Magnet brushless DC motor using finite element method Proceedings form *IEMDC* **32**(6) 241-5
[13] Hwang S M, Lieu D K 1995 Reduetion of torque ripple in brushless DC motors *IEEE Trans on Magneties* **31**(6) 3737-39
[14] Kim Yoon-Ho, Kook Yoon-Sang, Ko Yo 1997 A new technique of reducing torque ripples for BLDCM drives *IEEE Trans.on Industrial Electronics* **44**(5) 735-9
[15] Kim Yoon-Ho, Cho Byung-Guk, Ko Yo 1994 Generalized techniques of reducing torque ripples in BLDCM drives *Proceedings from IECON* **21**(2) 514-9

Authors

Zhang Jiong, born in February, 1978, Liuzhou County, Guangxi Province, P.R. China

Current position, grades: lecturer of School of Vocational and Technical Education, Guangxi University of Science and Technology, China.
University studies: B.Sc. in College of mechanical and power engineering from Chongqing University of Science and Technology in China. M.Sc. from Chongqing University in China.
Scientific interest: Manufacturing Engineering and Automation, Materials processing engineering.
Publications: more than 10 papers published in various journals.
Experience: teaching experience of 7 years, 5 scientific research projects.

Chen Shaofei, born in March, 1981, Liuzhou County, Guangxi Province, P.R. China

Current position, grades: lecturer of School of Engineering Training Center, Guangxi University of Science and Technology, China.
University studies: B.Sc. in Electrical Engineering and Automation from Hefei University of technology in China. M.Sc. from Chongqing University in China.
Scientific interest: Control theory and control engineering, Electrical and electronic science.
Publications: more than 4 papers published in various journals.
Experience: teaching experience of 4 years, 3 scientific research projects.

Liu Lihua, born in March, 1981, Liuzhou County, Guangxi Province, P.R. China

Current position, grades: lecturer of School of College of Science, Guangxi University of Science and Technology, China.
University studies: B.Sc. in College of Science from Guangxi University of Science and Technology in China. M.Sc. from Guilin university of electronic in China.
Scientific interest: Management and optimization control, Management science.
Publications: more than 5 papers published in various journals.
Experience: teaching experience of 7 years, 4 scientific research projects.